Research Square

Preprints are preliminary reports that have not undergone peer review.
They should not be considered conclusive, used to inform clinical practice,
or referenced by the media as validated information.

A new perspective on the stratospheric polar vortex, sudden warmings and the ENSO modulation

Froila M. Palmeiro

froipalm@ucm.es

CMCC Foundation - Euro-Mediterranean Center on Climate Change

Bianca Mezzina

European Centre for Medium Range Weather Forecasts (ECMWF)

Javier García-Serrano

Universitat de Barcelona (UB)

Perspective

Keywords:

Posted Date: October 30th, 2026

DOI: https://doi.org/10.21203/rs.3.rs-11307442/v1

License: This work is licensed under a Creative Commons Attribution 4.0 International License.
Read Full License

Additional Declarations: No competing interests reported.

A new perspective on the stratospheric polar vortex, sudden warmings and the ENSO modulation

Froila M. Palmeiro[1,2], Bianca Mezzina[3,4] and Javier García-Serrano[5]

[1]Instituto de Geociencias (IGEO), Consejo Superior de Investigaciones Científicas Universidad Complutense de Madrid, Madrid, Spain

[2]CMCC Foundation - Euro-Mediterranean Center on Climate Change, Italy

[3]European Centre for Medium Range Weather Forecasts (ECMWF), Bonn, Germany

[4]Université catholique de Louvain, Earth and Life Insitute, Louvain-La-Neuve, Belgium

[5]Group of Meteorology, Universitat de Barcelona (UB), Barcelona, Spain

Corresponding author: Froila M. Palmeiro (froipalm@ucm.es)

ABSTRACT

Circulation anomalies in the stratosphere, and particularly sudden stratospheric warmings (SSWs), have a strong impact on climate predictability at subseasonal-to-seasonal timescales. Understanding the effects of El Niño-Southern Oscillation on the occurrence and typology of SSWs remains a challenge. Here, we re-diagnose the three-dimensional structure of the stratospheric polar vortex by analysing relative vorticity – the local spinning motion of the flow – and show that it is characterised by strong positive (cyclonic) vorticity over the pole with two regions of maximum rotation that can be traced as two columns down to the troposphere, one over northern Canada and the other over Eurasia. During El Niño, enhanced wave activity over the eastern North Pacific acts as a source of negative (anticyclonic) vorticity in the upper troposphere, weakening the Canadian maximum; hence, the polar vortex appears displaced over Eurasia, favouring displacement-type SSWs. During La Niña, strengthened positive (cyclonic) vorticity over northern Canada, reinforcing the Canadian column of rotation, results in an elongated polar vortex with two well-separated centres of similar amplitude, facilitating split-type SSWs. Our results offer a novel framework for interpreting troposphere-stratosphere interaction and enhancing prediction skill of SSW events.

The North American-European winter climate can be heavily affected by changes in the stratospheric polar vortex (SPV), a cold air mass encircled by strong westerly winds that dominate the extratropical atmosphere above 10–15 km[1]. In particular, abrupt disruptions of the SPV, called sudden stratospheric warmings (SSWs)[2], occurring roughly every other winter, can lead to cold air outbreaks, severe storms, and extreme weather conditions that can last for weeks with dramatic economic and human damages[3]. The SPV and its variability, including SSWs, can, in turn, be influenced by remote drivers such as El Niño–Southern Oscillation (ENSO), a linkage that is well-known but whose exact mechanisms are still not settled[4]. The traditional viewpoint of the ENSO impact on the polar stratosphere is typically diagnosed in the zonal-mean framework and described as increased wave propagation during El Niño, which is triggered by the deepening of the Aleutian Low and weakens the polar vortex; while the opposite—weakening of the Aleutian Low and reduced upward wave propagation—would occur during La Niña, which strengthens the polar vortex[4,5].

Given this seasonal-mean effect of ENSO on the polar vortex strength, there is also an expected impact on the frequency of SSWs[6,7]. Although SSWs appear to be more likely during El Niño in climate models[8,9], results from observations are inconclusive, and in the last seven decades, SSWs have indeed occurred more frequently during La Niña[10]. Considering the time-dependence of the ENSO influence on the stratosphere[11,12], and the full establishment of the ENSO-forced Rossby wavetrain in the troposphere[13], it is not surprising that ENSO can modulate the timing of SSWs even if the total, wintertime occurrence is unchanged[10]. Moreover, previous studies have highlighted that ENSO and SSWs should be considered as different sources of variability for the SPV, given the longer, seasonal timescale of the ENSO signal as compared to the shorter, daily-weekly SSW signal[7,10,14].

ENSO could also favour certain types of polar vortex disruptions, in a way that SSWs during El Niño typically manifest as a displacement of the polar vortex away from the pole (wave-1), whereas split-type events (wave-2) seem to be favoured during La Niña[15]. However, the proposed mechanisms to explain the impact of ENSO on SSWs through changes in the upward wave injection to the stratosphere are reduced to the zonal-mean framework, which makes it difficult

to reconcile the different impacts of El Niño and La Niña on the polar vortex preconditioning of a particular SSW type.

Earlier studies have made valuable contributions to characterize the two-dimensional structure of the polar vortex using elliptical diagnostics in the potential vorticity field[16,17]. Later, they were explicitly used to define geometric moments to differentiate displacement and split SSWs[18,19], or even using other simpler variables such as geopotential height[20]. While the typical description of the polar vortex is that of an area of low pressure and high rotation (vorticity) over the pole, two main centres of maximum vorticity can actually be identified in the lower stratosphere, which have not yet been documented in the literature. In this study, we thoroughly examine the vertical structure of these two rotation centres, with a novel description in the three-dimensional relative vorticity field, and put it into practice to diagnose and interpret the ENSO–polar vortex relationship from a simple, innovative approach. A better understanding of this linkage is essential to shed light on the triggering and dynamics of SSWs.

Climatological structure of the stratospheric polar vortex

Fig. 1 shows the life cycle of the stratospheric polar vortex climatology using relative vorticity at several timesteps from October to March during ENSO-neutral years, April can be found in Extended Data Fig. 1., and a complete animation on a daily timescale can be accessed in Supplementary Video 1. In early winter, the strongest rotation begins in the middle-upper stratosphere and the vortex penetrates deeper into lower levels as winter progresses. During November–December, the maximum rotation at 10 hPa collocates over Siberia (Fig. 1, top-right panels), but from January onwards, it shifts ~45° clockwise and expands westwards, forming a distorted elliptical shape that elongates along the 90°W–90°E longitudinal axis in the middle stratosphere (10 hPa). This structure features two centres of maximum relative vorticity, which vertically appear as two distinct columns of rotation (Fig. 1, left panels), consistent with previous vortex visualisations[19]. As these centres are located over Eurasia and northern Canada, they will hereafter be referred to as the Eurasian and Canadian centres, respectively.

This time evolution can also be tracked by the eddy geopotential-height field (10 hPa; Fig. 1, bottom-right panels), illustrating zonal asymmetries of the background flow. During November–December, the polar vortex projects on a purely wave-1 structure in the middle stratosphere, with positive anomalies over the North Pacific (i.e. the Aleutian High[21,22]) and its negative counterpart over Eurasia (i.e. the polar vortex). This dipole appears clockwise rotated in mid-winter, with its negative centre further expanding westwards. Indeed, a secondary lobe of cyclonic circulation, initiated in January, is fully settled in February over northern Canada, representing the Canadian column of the polar vortex. These different structures are consistent with the vertical evolution of the polar vortex through winter, when periods of coupling between the stratosphere and the troposphere become evident (Supplementary Video 1). Interestingly, while coupling through the Eurasian column can occur during the entire winter, the interaction over northern Canada appears more restricted to mid-late winter, namely from January onwards.

The climatology of the main regions of upward wave propagation (i.e. wave injection) reveals interesting features regarding the polar vortex structure and its evolution (Extended Data Fig. 2). The largest wave injection from the lower stratosphere, measured by the eddy heat flux at 100 hPa, occurs over the Aleutian region[23] and reaches its maximum in January–February (bottom panel, red), concurrent with the westward shift of the polar vortex and the strengthening of the Canadian column, thereby suggesting causality. In contrast, the other documented area of large wave injection is over northern Europe–Siberia[24], right where the Eurasian column of the polar vortex collocates throughout the winter, showing a climatological evolution that is mostly constant from early winter to late winter (bottom panel, yellow). The latter is in agreement with the more regular and continuous coupling observed for the Eurasian column, as discussed above.

ENSO modulation of the stratospheric polar vortex

Considering that the ENSO effect on the polar stratosphere is maximum during mid-winter (January–February[11,25]), this two-month period represents the target season to explore the ENSO–polar vortex relationship.

When El Niño and La Niña winters are considered separately (Fig. 2, top), the most notable difference in the polar vortex structure at 10 hPa lies in the strength of the Canadian centre, which is weakened during El Niño but reinforced during La Niña. This impact is associated with a displacement of the polar vortex towards Eurasia during El Niño, whereas the opposite occurs during La Niña: the Canadian centre intensifies, causing the maximum rotation to elongate, and the two centres to become comparable in amplitude. The strengthening of the Canadian centre is also evident at lower levels (Fig. 2, middle), resulting in two similar columns of relative vorticity during La Niña (Extended Data Fig. 3).

The mechanism underlying the modulation of the Canadian lobe of the polar vortex appears to be in the troposphere, triggered by the extratropical response to ENSO, which results in a Rossby wavetrain crossing the North Pacific–American sector into the North Atlantic[26,27,28]. Fig. 2 (bottom) shows this ENSO-forced wavetrain in the lower stratosphere (200 hPa; shading) together with the background, stationary wave pattern (i.e. composite full-field eddy; red/blue contours) for El Niño and La Niña; superimposed with black contours is the polar vortex based on relative vorticity at 10 hPa (also in Fig. 2, top). Over North America–Canada, El Niño yields high-pressure anomalies (red shading), which collocate with the lowermost part of the Canadian column, providing anticyclonic torque and thus contributing to the polar vortex weakening from below. In contrast, La Niña displays low-pressure anomalies (blue shading) and cyclonic circulation, which reinforces the Canadian column of rotation and strengthens the polar vortex in the lower-middle stratosphere.

ENSO modulation of SSWs: displacement vs split

To explore the evolution of the polar vortex structure during SSWs, the analysis is now focused on daily timescales. According to previous studies, SSWs in El Niño winters resemble a displacement from the pole towards Eurasia and project onto a wave-1 pattern, while they show a split-type signal with a larger wave-2 component for La Niña[8,15,29]. In our framework, the dynamics leading to such distinct behaviours can be further diagnosed by examining the 10-hPa

relative vorticity during the preconditioning phase of SSWs (Fig. 3, top). For El Niño winters, the 10-day period before SSWs shows an isolated vortex of rotation clearly displaced from the pole. The time evolution of the polar vortex in the [–20, 5]-day period around the SSW central date (Supplementary Video 3) depicts the progressive weakening of the polar vortex and its confinement over Eurasia. This SSW pattern is reminiscent of an extreme state of the seasonal-mean effect of El Niño (Fig. 2, top left). On the other hand, the seasonal-mean strengthening of the Canadian column during La Niña (Fig. 2, top right) results in a more elliptical, elongated polar vortex, and when sufficient intraseasonal instability is reached[30,31], the polar vortex ultimately divides into two cyclonic vortices, leading to a split. This other SSW pattern is also evident at lower levels (Fig. 3, middle; Extended Data Fig. 4, and Supplementary Video 3). The results illustrate how different ENSO preconditioning via the strength of the Canadian column likely determines the type of SSW finally occurring during El Niño/La Niña winters. Note that this preconditioning might not necessarily translate into a different frequency of occurrence, as most of the intraseasonal wave activity reaching the middle stratosphere is unrelated to ENSO[7,10,23,29,30,31,32,33]; here evidenced by similar eddy heat-flux anomalies over the Aleutian and Eurasian regions (Fig. 3, bottom).

Implications of the SPV structure

The three-dimensional analysis of relative vorticity provides a detailed description of the stratospheric polar vortex rotation and its evolution through the winter. While in the middle-upper stratosphere, the polar vortex is centered over the pole, rotation in the middle-lower stratosphere can be traced to particular locations, mainly occurring over Eurasia throughout the winter, with a second centre establishing over Canada in mid-winter (Fig. 1). The distinction between these two columns of rotation sets the basis for our interpretation of how El Niño and La Niña modify the morphology of the polar vortex by modulating its Canadian maximum (see the schematic diagram in Fig. 4).

The modulation of the tropospheric Aleutian Low associated with ENSO is currently the most common dynamical explanation for its impact on the polar vortex[4]. However, earlier studies had pointed at the centre of action over Canada as a key factor instead[34,35,36,37], which becomes the stratospheric Aleutian High[21,38]. The crucial role of this anomalous circulation over Canada, which for El Niño is opposite in sign to the polar vortex, was highlighted in later studies[25,39,40] and recently revamped by Mezzina et al.[41]. Our study supports the hypothesis that the Canadian centre of action plays a dominant role in the ENSO–polar vortex teleconnection and provides a straightforward interpretation for its mechanism. By accounting for the three-dimensional structure of the polar vortex in mid-late winter—specifically the location of its two low-level centres of positive vorticity—it is plausible that the ENSO-forced wavetrain over that region directly modulates the strength of the polar vortex on that flank (Figs. 2 and 4). Although this linear approach is consistent with the well-documented zonal-mean response to ENSO[41], we additionally identify northern Canada as a key location for troposphere–stratosphere coupling at interannual timescales.

Also, beyond the stationary, seasonal-mean impact of ENSO on the polar vortex strength, our approach provides a straightforward interpretation of the preference for wave-1 SSWs during El Niño and wave-2 SSWs during La Niña (Figs. 3 and 4). It is to note that this is the first dynamical view reconciling the apparently counterintuitive evidence[4] that La Niña can strengthen the polar vortex while simultaneously boosting the occurrence of SSWs.

Finally, rather than attempting to establish a new methodology for characterising the polar vortex and its variability, this study offers a simpler perspective on the polar vortex structure that complements the traditional zonal-mean paradigm. It offers a new path towards assessing and (possibly) improving the representation of the stratospheric polar vortex in climate models. For instance, a poor representation of the Canadian column of rotation may lead to a misrepresented polar vortex response to ENSO, even if the tropospheric ENSO response is realistic, as found in recent studies[41,42]. Likewise, the persistent challenge that models face in simulating the wave-2 component of the flow as well as vortex splits[43,44] may stem from the same misrepresentation of the Canadian column of rotation, considering its major role in setting the wave-2 SSW pattern.

Our approach expands the diagnosis and understanding of the processes involved in stratospheric circulation variability, particularly SSWs, as in other recent studies[45]. As such, it may eventually contribute to enhanced prediction of the occurrence of SSWs, and ultimately their impact on tropospheric circulation and surface climate.

REFERENCES

1. Manney, G. L., Zurek, R. W., O'Neill, A. & Swinbank, R. On the motion of air through the stratospheric polar vortex. J. Atmos. Sci. 51, 2973–2994 (1994).
2. Baldwin, M. P. et al. Sudden stratospheric warmings. Rev. Geophys. 59, e2020RG000708 (2021).
3. Domeisen, D. I. & Butler, A. H. Stratospheric drivers of extreme events at the Earth's surface. Commun. Earth Environ. 1, 59 (2020).
4. Domeisen, D. I. et al. The role of the stratosphere in subseasonal to seasonal prediction: 1. Predictability of the stratosphere. J. Geophys. Res. Atmos. 124, 4500–4522 (2019).
5. Iza, I. & Calvo, N. Role of stratospheric resolution in the tropical Pacific SST impact on the Northern Hemisphere polar vortex. Clim. Dyn. 44, 2401–2415 (2015).
6. Butler, A. H., Polvani, L. M. & Deser, C. Separating the stratospheric and tropospheric pathways of El Niño–Southern Oscillation teleconnections. Environ. Res. Lett. 9, 024014 (2014).
7. Oehrlein, J., Chiodo, G. & Polvani, L. M. Separating and quantifying the distinct impacts of El Niño and sudden stratospheric warmings on North Atlantic and Eurasian wintertime climate. Atmos. Sci. Lett. 20, e923 (2019).
8. Taguchi, M. & Hartmann, D. L. Increased occurrence of stratospheric sudden warmings during El Niño as simulated by WACCM. J. Clim. 19, 324–332 (2006).
9. Trascasa-Castro, P., Ineson, S., Maycock, A. C., Dunstone, N. J. & Scaife, A. A. The climate response to El Niño in the North Atlantic–European region in CMIP5. J. Clim. 32, 8611–8631 (2019).

10. Palmeiro, F. M., García-Serrano, J., Ruggieri, P., Batté, L. & Gualdi, S. On the influence of ENSO on sudden stratospheric warmings. J. Geophys. Res. Atmos. 128, e2022JD037607 (2023).
11. Ineson, S. & Scaife, A. A. The role of the stratosphere in the European climate response to El Niño. Nat. Geosci. 2, 32–36 (2009).
12. Ayarzagüena, B., Ineson, S., Dunstone, N. J., Baldwin, M. P. & Scaife, A. A. Intraseasonal effects of El Niño–Southern Oscillation on North Atlantic climate. J. Clim. 31, 8861–8873 (2018).
13. Bladé, I., Newman, M., Fortuny, D. & Sardeshmukh, P. D. Diagnosing the regional tropospheric response to ENSO. J. Clim. 21, 2697–2711 (2008).
14. Polvani, L. M., Sun, L., Butler, A. H., Richter, J. H. & Deser, C. Distinguishing the surface impacts of El Niño and stratospheric sudden warmings. Geophys. Res. Lett. 44, 5674–5682 (2017).
15. Barriopedro, D. & Calvo, N. On the relationship between ENSO, stratospheric sudden warmings, and blocking. J. Clim. 27, 4704–4720 (2014).
16. Waugh, D. W. Elliptical diagnostics of stratospheric polar vortices. Q. J. R. Meteorol. Soc. 123, 1725–1748 (1997).
17. Waugh, D. W. & Randel, W. J. Climatology of Arctic and Antarctic polar vortices using elliptical diagnostics. J. Atmos. Sci. 56, 1594–1613 (1999).
18. Mitchell, D. M., Charlton-Perez, A. J. & Gray, L. J. Characterizing the variability and extremes of the stratospheric polar vortices using 2D moment analysis. J. Atmos. Sci. 68, 1194–1213 (2011).
19. Lawrence, Z. D. & Manney, G. L. Characterizing stratospheric polar vortex variability with computer vision techniques. J. Geophys. Res. Atmos. 123, 1510–1535 (2018).
20. Seviour, W. J., Mitchell, D. M. & Gray, L. J. A practical method to identify displaced and split stratospheric polar vortex events. Geophys. Res. Lett. 40, 5268–5273 (2013).
21. Harvey, V. L. & Hitchman, M. H. A climatology of the Aleutian High. J. Atmos. Sci. 53, 2088–2101 (1996).

22. Colucci, S. J. & Ehrmann, T. F. Aleutian anticyclones and stratospheric sudden warmings. J. Atmos. Sci. 75, 2741–2755 (2018).
23. Garfinkel, C. I., Hartmann, D. L. & Sassi, F. Tropospheric precursors of anomalous Northern Hemisphere stratospheric polar vortices. J. Clim. 23, 3282–3299 (2010).
24. Newman, P. A. & Nash, E. R. Quantifying the wave driving of the stratosphere. J. Geophys. Res. Atmos. 105, 12485–12497 (2000).
25. Manzini, E., Giorgetta, M. A., Esch, M., Kornblueh, L. & Roeckner, E. The influence of sea surface temperatures on the northern winter stratosphere: Ensemble simulations with the MAECHAM5 model. J. Clim. 19, 3863–3881 (2006).
26. Hoskins, B. J. & Karoly, D. J. The steady linear response of a spherical atmosphere to thermal and orographic forcing. J. Atmos. Sci. 38, 1179–1196 (1981).
27. Horel, J. D. & Wallace, J. M. Planetary-scale atmospheric phenomena associated with the Southern Oscillation. Mon. Weather Rev. 109, 813–829 (1981).
28. Trenberth, K. E., Branstator, G. W., Karoly, D., Kumar, A. & Lau, N. C. Progress during TOGA in understanding and modeling global teleconnections associated with tropical sea surface temperatures. J. Geophys. Res. Oceans 103, 14291–14324 (1998).
29. Garfinkel, C. I., Shaw, T. A., Hartmann, D. L. & Waxman, N. N. The influence of the extratropical troposphere in driving stratospheric vortex sudden warmings. J. Atmos. Sci. 69, 2088–2099 (2012).
30. Birner, T. & Albers, J. R. Sudden stratospheric warmings and anomalous upward wave activity flux. SOLA 13, 8–12 (2017).
31. de la Cámara, A., Birner, T. & Albers, J. R. Are sudden stratospheric warmings preceded by anomalous tropospheric wave activity? J. Clim. 32, 7173–7189 (2019).
32. Orsolini, Y. J., Pavan, V. & Sopracordevole, G. Extreme flow events in the Northern Hemisphere winter stratosphere. Q. J. R. Meteorol. Soc. 135, 149–158 (2009).
33. Martius, O., Polvani, L. M. & Davies, H. C. Blocking precursors to stratospheric sudden warming events. Geophys. Res. Lett. 36, L14806 (2009).

34. van Loon, H. & Labitzke, K. The Southern Oscillation. Part V: The anomalies in the lower stratosphere of the Northern Hemisphere in winter and a comparison with the Quasi-Biennial Oscillation. Mon. Weather Rev. 115, 357–369 (1987).
35. Hamilton, K. A general circulation model simulation of El Niño effects in the extratropical Northern Hemisphere stratosphere. Geophys. Res. Lett. 20, 1803–1806 (1993).
36. Hamilton, K. An examination of observed Southern Oscillation effects in the Northern Hemisphere stratosphere. J. Atmos. Sci. 50, 3468–3474 (1993).
37. Hamilton, K. Interannual variability in the Northern Hemisphere winter middle atmosphere in control and perturbed experiments with the GFDL SKYHI general circulation model. J. Atmos. Sci. 52, 44–66 (1995).
38. Harvey, V. L. et al. On the 3D structure of the stratospheric polar vortex and Aleutian High. J. Atmos. Sci. 59, 2873–2887 (2002).
39. Baldwin, M. P. & O'Sullivan, D. Stratospheric effects of ENSO-related tropospheric circulation anomalies. J. Clim. 8, 649–667 (1995).
40. Sassi, F., Kinnison, D., Boville, B. A., Garcia, R. R. & Roble, R. Effect of El Niño–Southern Oscillation on the dynamical, thermal, and chemical structure of the middle atmosphere. J. Geophys. Res. Atmos. 109, D17108 (2004).
41. Mezzina, B. et al. Reassessing the role of the Aleutian Low in the ENSO teleconnection to the stratosphere. J. Clim. 35, 6101–6119 (2022).
42. Shen, X., Kretschmer, M. & Shepherd, T. G. A forensic investigation of climate model biases in teleconnections: The case of the relationship between ENSO and the northern stratospheric polar vortex. J. Geophys. Res. Atmos. 129, e2024JD041252 (2024).
43. Hall, R. J., Mitchell, D. M., Seviour, W. J. & Wright, C. J. Persistent model biases in the CMIP6 representation of stratospheric polar vortex variability. J. Geophys. Res. Atmos. 126, e2021JD034759 (2021).
44. Chávez-Pérez, V. M., Añel, J. A., Almaguer-Gómez, C. & de la Torre, L. Influence of satellite and presatellite periods on the validation of major sudden stratospheric warmings in historical CMIP5 simulations. Atmosphere 16, 628 (2025).

45. Davies, H. C. & Sprenger, M. Cyclone-like features within the stratospheric polar-night vortex. Geophys. Res. Lett. 51, e2024GL109529 (2024).

Methods

Atmospheric fields from the ERA5 reanalysis[1] have been analysed, using hourly data to calculate daily values and also monthly data. This includes relative vorticity to represent the stratospheric polar vortex, geopotential height at 200 hPa, zonal-mean zonal wind at 10 hPa to detect Sudden Stratospheric Warmings (SSWs), and the product of meridional wind and temperature (v*T*) at 100 hPa to derive the meridional zonal-eddy heat flux. El Niño and La Niña events are identified using the Relative Oceanic Niño Index (RONI[2]) when the December–January–February (DJF) mean index reached or exceeded 1 °C for El Niño or fell to or below -0.9 °C for La Niña, to include the same number of events in each category. This results in the following El Niño winters: 1963, 1965, 1968, 1972, 1976, 1977, 1982, 1986, 1991, 1994, 1997, 2009 and 2015; and La Niña winters: 1970, 1973, 1975, 1988, 1995, 1998, 1999, 2005, 2007, 2008, 2010, 2017 and 2020. SSWs are defined as reversals of the zonal-mean zonal wind at 10 hPa to easterlies at any latitude between 55°N and 70°N[3] from the 1 November to 11 March with at least 21 days of westerly-wind separation between consecutive events. For this analysis we only consider SSWs from January onwards, which yields 8 SSWs during El Niño and 9 during La Niña. Statistical significance is evaluated using a 1,000-trial Monte Carlo tests. Three-dimensional visualizations were generated using ParaView[3] (v2.3) in combination with the pv_atmos code[4,5].

Data availability

The ERA5 dataset used in this study is publicly available from the European Centre for Medium-Range Weather Forecasts (ECMWF) via the Copernicus Climate Change Service (C3S). The data can be accessed via the Copernicus Climate Data Store (CDS)1 under the terms and conditions provided on the CDS website. The RONI index can be found at the NOAA Climate Prediction Center website (https://www.cpc.ncep.noaa.gov/products/analysis_monitoring/enso/roni/#).

References

1. Hersbach, H. et al. ERA5 hourly data on single levels from 1940 to present. Copernicus Climate Change Service (C3S) Data Store (2023).

2. L'Heureux, M. L. *et al.* A relative sea surface temperature index for classifying ENSO events in a changing climate. *J. Clim.* **37**, 1197–1211 (2024).

3. Palmeiro, F. M., Barriopedro, D., García-Herrera, R. & Calvo, N. Comparing sudden stratospheric warming definitions in reanalysis data. *J. Clim.* **28**, 6823–6840 (2015).

4. Ahrens, J., Geveci, B. & Law, C. ParaView: An end-user visualization tool. The Visualization Handbook 824, 502-531 (2005).

5. Jucker, M. pv_atmos: A ParaView plugin for atmospheric sciences. Zenodo https://doi.org/10.5281/zenodo.12879 (2014).

6. Jucker, M. pv_atmos: v2.3. Zenodo https://doi.org/10.5281/zenodo.34127 (2015).

Acknowledgements

The authors thank Tim Stockdale for his constructive comments on an earlier draft of this paper.

Author contributions

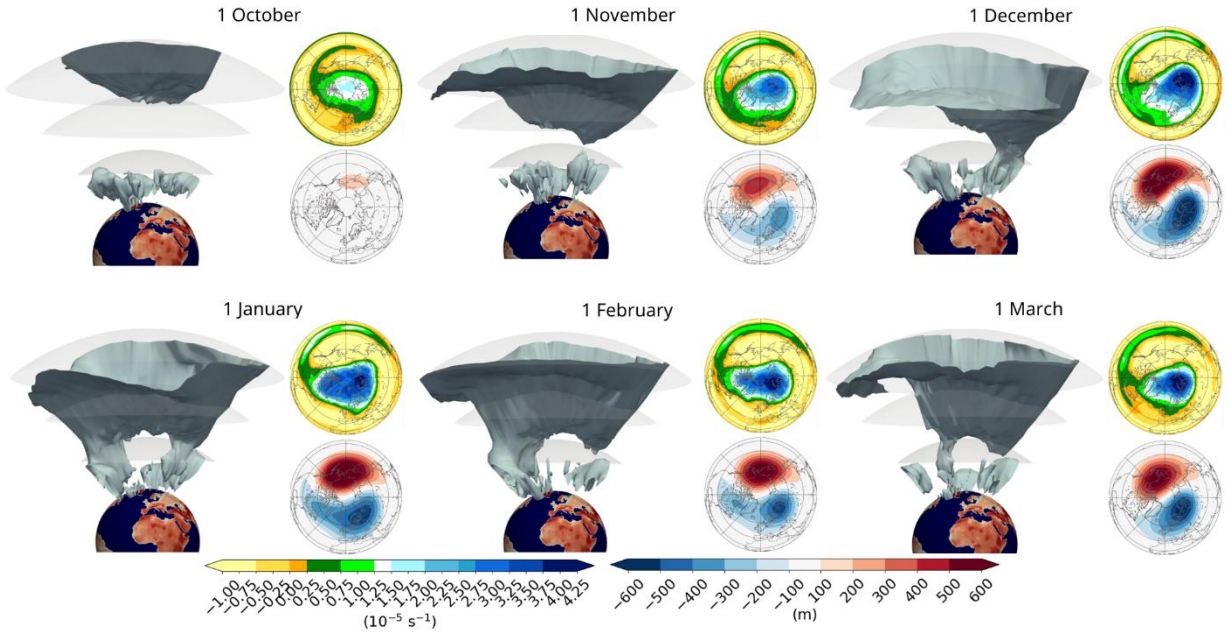
FMP prepared the manuscript and designed the figures and video files. BM wrote the introduction and designed the schematic. FMP, BM and JGS revised and edited the manuscript.

Funding Statements

FMP was supported by the European Union's Horizon Europe Research and Innovation Programme under the Marie Skłodowska-Curie Grant Agreement No. 101065820. This study received funding from the Spanish SESHAT project (PID2024-159949NA-I00). BM was a Fonds de la Recherche Scientifique—FNRS (F.R.S.–FNRS) postdoctoral researcher during the first phase of the study and was later supported by the European Union Horizon Europe project ASPECT (Grant Agreement No 101081460).

Competing interests

The authors declare no competing interests.



354

355 **Fig. 1**: **The stratospheric polar vortex life cycle**. Snapshots of the climatological stratospheric
356 polar vortex evolution from October to March for the first day of each month during non-ENSO
357 years. For each panel, left: surface contour of relative vorticity ($1.8x10^{-5}$ s^{-1}), quasi-transparent
358 layers correspond to 100, 10 and 1 hPa pressure levels; upper-right: relative vorticity at 10 hPa;
359 bottom-right: zonal-eddy-component of full-field geopotential height at 10 hPa. A complete
360 visualization of the vortex evolution can be accessed in Supplementary Video. 1.

361

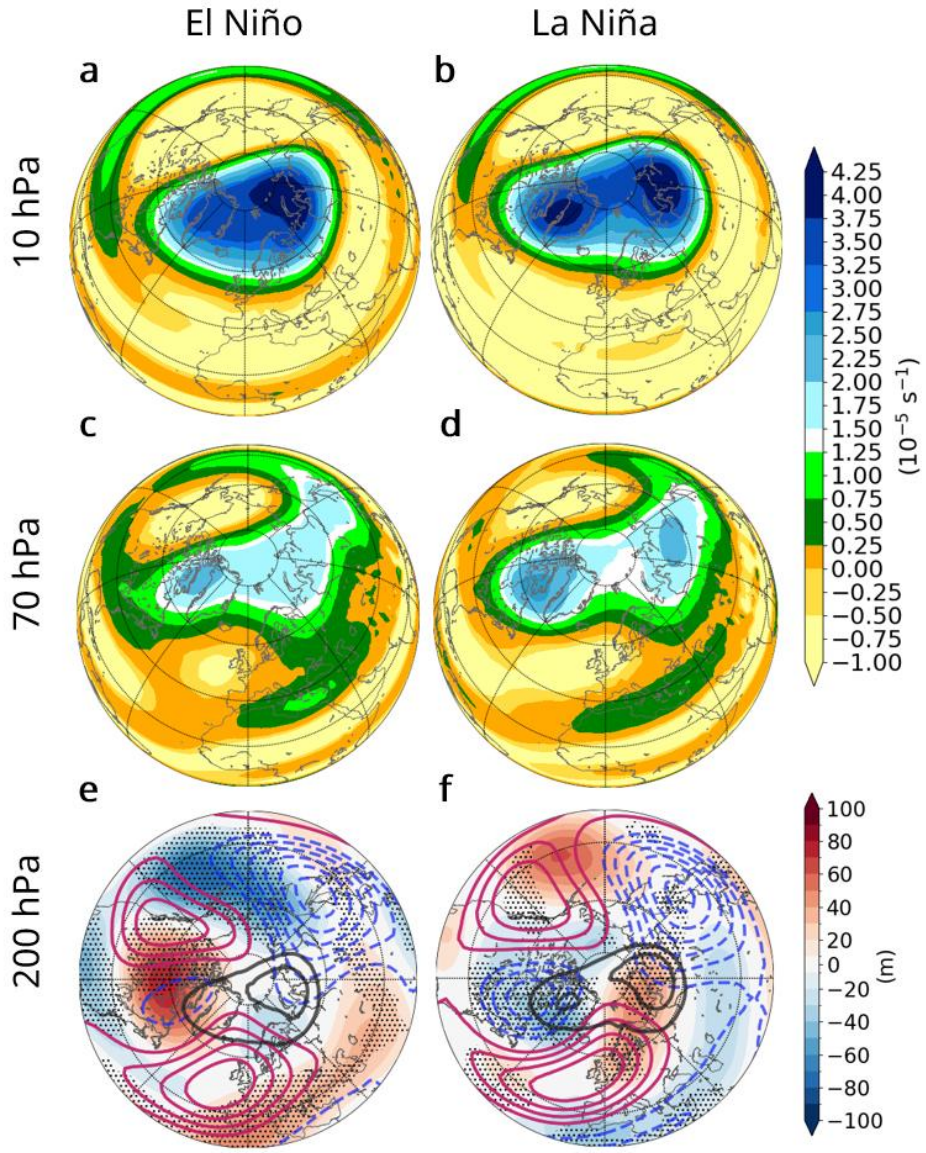


Fig. 2: Modulation of the stratospheric polar vortex structure during El Niño and La Niña. Composite of relative vorticity during El Niño (left) and La Niña (right) winters at 10 hPa (a, b) and 70 hPa (c, d). Bottom panels: geopotential height anomalies at 200 hPa (shading), zonal-eddy component of full-field geopotential height at 200 hPa (coloured contours, red: positive - blue: negative; c.i. 50 m), and relative vorticity (black contours: 2.5×10^{-5} and 3.5×10^{-5} s^{-1} ; same as in panels a,b) during El Niño (e) and La Niña (f) winters. Statistically significant areas at 95% confidence level according to a 1,000-trial Monte Carlo test are stippled in panels (e, f).

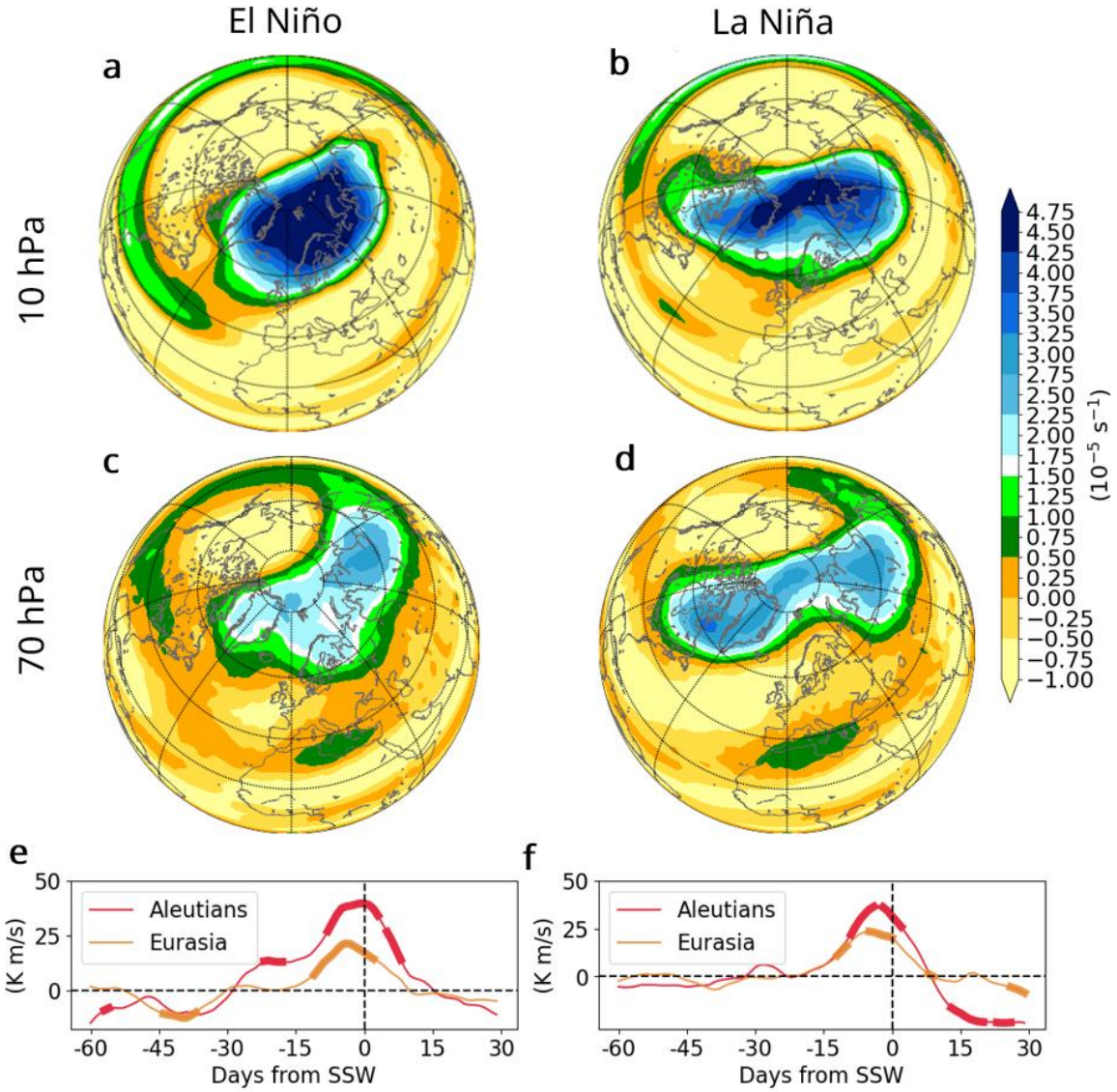
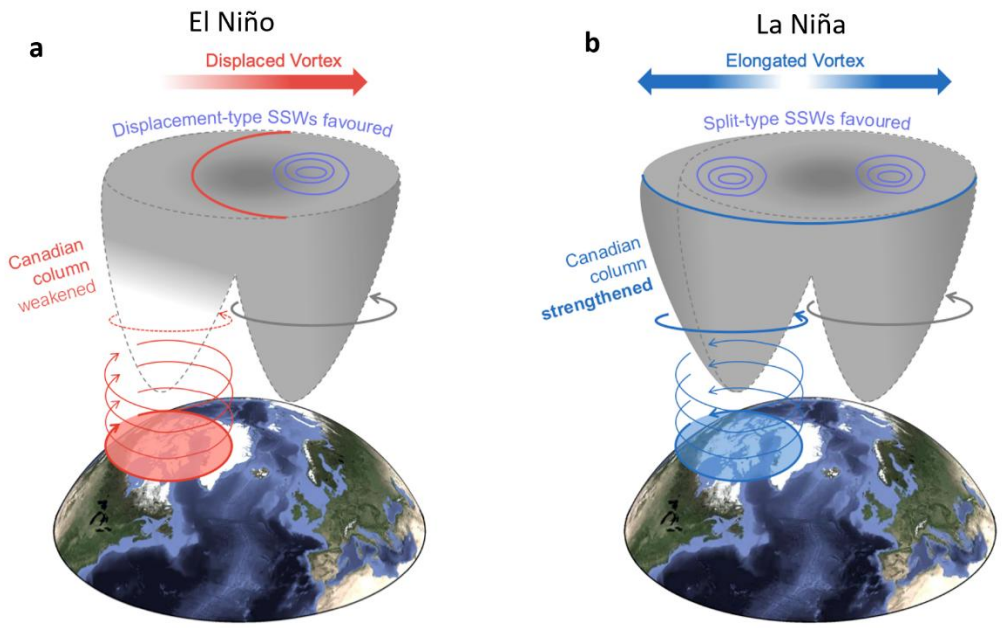


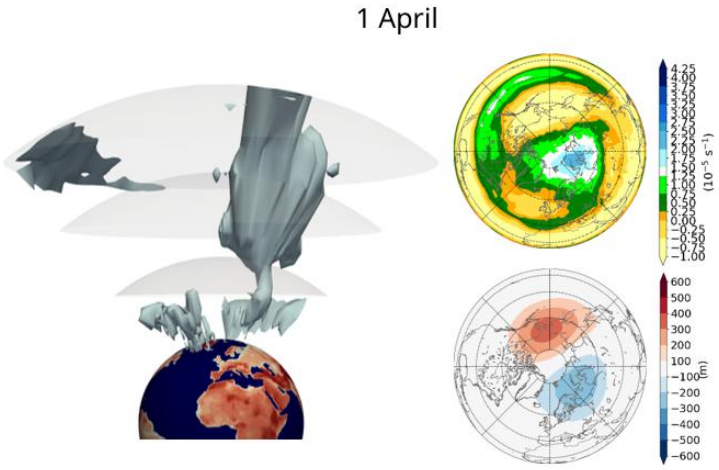
Fig. 3: Preconditioning of the sudden stratospheric warming structure during El Niño and La Niña. Composite of relative vorticity averaged over the week before SSWs during El Niño (left) and La Niña (right) winters at 10 hPa (a, b) and 70 hPa (c, d). Bottom panels: eddy heat flux at 100 hPa averaged over the Aleutian region 135°E-135°W / 55°N-85°N (red) and the Eurasian region 55°N-75°N / 0°E-135°E (orange). An animated version of (a,b) during the SSW occurrence can be accessed in Supplementary Video 2.



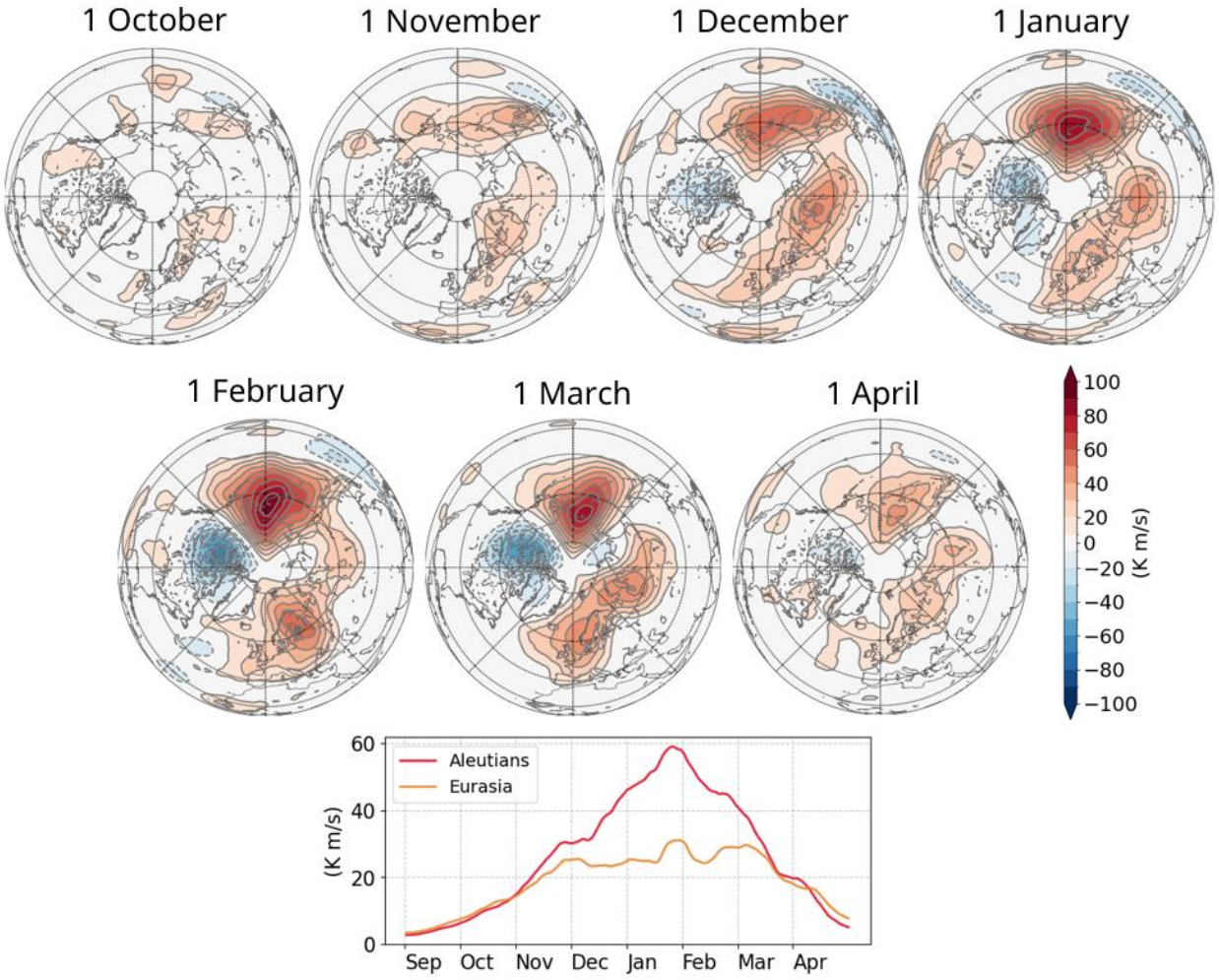
379
380

381 **Fig. 4: Schematic of the ENSO impact on the stratospheric polar vortex during El Niño and La**
382 **Niña.** The polar vortex is depicted in grey, with dashed lines representing its
383 climatological/neutral state and the grey arrow indicating the cyclonic rotation of the Eurasian
384 columns. The red and blue circles represent anomalous anticyclonic and cyclonic vorticity in the
385 upper troposphere – lower stratosphere, over the Canadian column, associated with El Niño and
386 La Niña, respectively. The red dashed arrow in (a) indicates the weakening of the Canadian
387 column related to El Niño, which results in the polar vortex being displaced over Eurasia (red thick
388 line) and favoured displacement-type SSWs. The thick blue arrow in (b) indicates that
389 the Canadian column of rotation is reinforced during La Niña, resulting in an elongated polar
390 vortex (blue thick line) and favoured split-type SSWs.
391

Extended Data

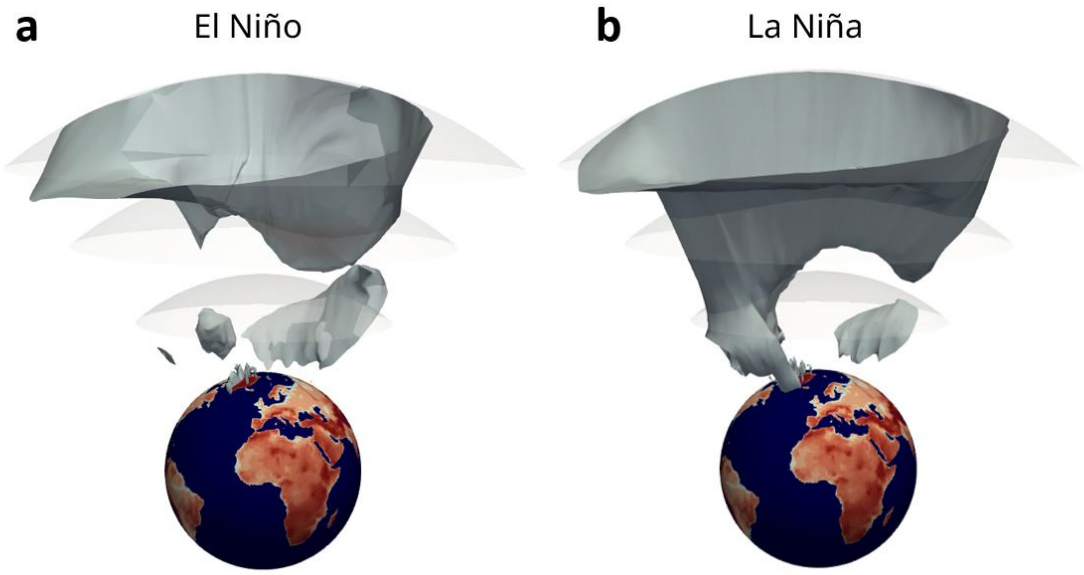


Extended Data Fig. 1. Same as in Fig. 1 but for April.



396

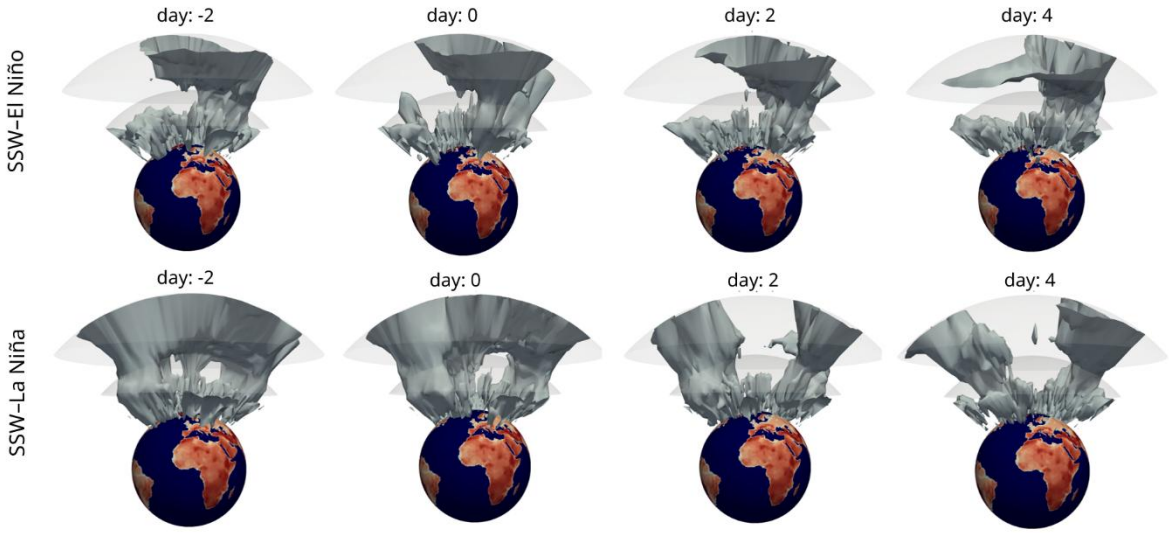
397 **Extended Data Fig. 2.** Climatological zonal-eddy heat flux from October to April at 100 hPa.
398 Bottom Panel: climatological zonal-eddy heat flux averaged over the Aleutian region 135°E-
399 135°W / 55°N-85°N (red) and the Eurasian region 55°N-75°N / 0°E-135°E (orange).



400

401 **Extended Data Fig. 3.** Composite of relative vorticity during (a) El Niño and (b) La Niña, surface
402 contour of relative vorticity is at $2x10^{-5}$ s^{-1}, quasi-transparent layers correspond to 100, 10 and 1
403 hPa pressure levels.

404



405

406 **Extended Data Fig. 4.** Snapshots of the SSW composite in the days, -2, 0, 2 and 4 of its occurrence;
407 during El Niño (top) and La Niña (bottom) winters. Surface contour of relative vorticity (1.8×10^{-5}
408 s^{-1}) is plotted, quasi-transparent layers correspond to 100 and 10 hPa pressure levels. A complete
409 visualization of the SSW evolution can be accessed in Supplementary Video. 3.

410

411 **Captions of Supplementary Videos**

412

413 **Supplementary Video 1.** Climatological stratospheric polar vortex evolution from October to
414 March during non-ENSO years. Surface contour of relative vorticity ($1.8x10^{-5}$ s^{-1}) is plotted, quasi-
415 transparent layers correspond to 100, 10 and 1 hPa pressure levels.

416

417 **Supplementary Video 2.** Composite of relative vorticity from 20 days before the SSW to 5 days
418 after, during El Niño (left) and La Niña (right) winters at 10 hPa.

419

420 **Supplementary Video 3.** Time evolution of the SSW composite from 20 days before the SSW to
421 5 days after during El Niño (left) and La Niña (right) winters. Surface contour of relative vorticity
422 ($1.8x10^{-5}$ s^{-1}) is plotted, quasi-transparent layers correspond to 100 and 10 hPa pressure levels.

Supplementary Files

This is a list of supplementary files associated with this preprint. Click to download.

- SupplementaryVideo2.gif
- SupplementaryVideo1.gif
- SupplementaryVideo3.gif